

Following sound through a crack

C.G. Don and G.G. Swenson

School of Physics, Monash University, Clayton, Victoria, AUSTRALIA

ABSTRACT

Gaps occur in many acoustic barriers and buildings, allowing sound to pass from one side to another. But exactly how does sound pass through a gap? Measuring the transmitted energy when continuous wave (CW) sound is incident on one side allows an estimate to be made of the energy passing through the crack, but does not permit a detailed analysis of the mechanisms involved. However, if a short duration pulse of sound is used, the transmitted sound exhibits a sequence of pulses in time, obviously linked in some way to various possible paths through the crack. At first sight it is tempting to associate these peaks with a set of modes, similar to those set up in an organ pipe. Unfortunately, simple calculations of path lengths and pulse delays demand an embarrassingly large speed of sound. Moreover, some of the transmitted pulses are significantly narrower than the incident pulse. Perhaps the gap is simply filtering out the lower frequencies - but then why are some pulses broader? A full explanation requires the use of a diffraction theory that provides both magnitude and phase information.

INTRODUCTION

Various studies have examined aperture behaviour in thick barriers, especially theoretical treatments, to establish the transmission loss or related variables in the frequency domain (Gomperts and Kihlman 1967, Sauter and Soroka 1970, Horner and Peat 2006). Alternatively, the use of acoustic pulses is a useful method of experimentally determining the insertion loss of wide barriers with hard or soft surfaces and also ones with “cracks” (Papadopoulos and Don 1991). Experimentally, when a pulse was transmitted through a gap a sequence of peaks occurred at the receiver, the nature of the sequence, depending on the gap geometry. Initially it was postulated that these peaks resulted from the formation of various “modes” within the gap, but this model gave rise to a number of unresolved problems (Don, Swenson and Butyn 1995). The acoustical properties of slit systems are difficult to evaluate theoretically over a wide frequency range, so we seek to explain and generate the observed pulse trains using a simple diffraction model and Snell’s law. Such information could then be used to calculate the insertion loss of complex systems without the need to resort to experimental measurements or computationally lengthy calculations. The insertion loss of slit systems can display significant minima at particular frequencies, hence the need to know the system properties over a wide frequency range to permit “tuned” filtering.

EXPERIMENTAL DESIGN

Barrier arrangement and pulse generation

To investigate experimentally the behaviour of wide barriers, an acoustic impulse generated by the discharge of an axially-symmetric shot-shell primer source was used as the probe, as in Figure 1. The barrier, formed from acoustically hard fibre board, was mounted with the diffracting edges vertical and measurements were taken on a plane 1.4m above the floor to maximise the delay from unwanted floor or ceiling reflections, which were then time isolated and eliminated. Both the source and receiver were kept 1.0m from the nearest diffracting edge and in these experiments ϕ was maintained at 60° . A “direct microphone” was mounted exactly the same path distance away from the source as the receiver microphone behind the barrier. Because of the source symmetry, this direct microphone recorded the magnitude and shape of the pulse that would have reached the receiver if the barrier was not present. If only the “fixed” barrier was present, the change in pulse shape between the direct pulse and that diffracted around the barrier, when converted into the frequency domain, permitted the real and imaginary impedance behaviour of the barrier to be measured experimentally over the range from about 100Hz to 20kHz. The earlier experimental results of Papadopoulos and Don were generally found to be in good agreement with theoretical predictions, particularly those obtained from Medwin’s approach which has the advantage of providing both the real and imaginary frequency components (Medwin 1981). The relatively long duration pulse produced when the source pulse is diffracted by the fixed wide barrier will be referred to as the “bare” component and occurs in most of the following cases. It is the first component to arrive at the receiver and has been subtracted from the received signal before considering any other components.

An earlier interpretation and problems

When a parallel-sided gap was formed between the fixed wide barrier and a second movable barrier of the same width, in this case 362mm, the signal recorded beyond the gap exhibited a series of peaks: typically a strong broad first peak followed by a sequence of narrower peaks with the excess pressure gradually diminishing in amplitude (Figure 2). A possible explanation of these peaks was that each corre-

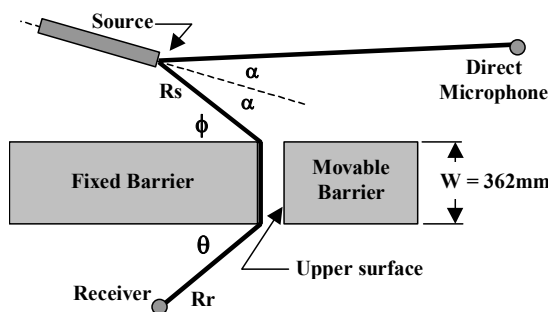


Figure 1. Experimental layout

sponded to a mode, formed in the gap, similar to those occurring in a resonating tube, where the extra path length of higher modes would be related to the delay of the peak. Graphing the delay time against the extra distance of the mode path revealed that the data for various gap widths fell on almost the same straight line, but the gradients indicated very high wave-speeds, varying from $360 \pm 5 \text{ms}^{-1}$ for a 30mm gap up to $395 \pm 10 \text{ms}^{-1}$ for a 100mm gap.

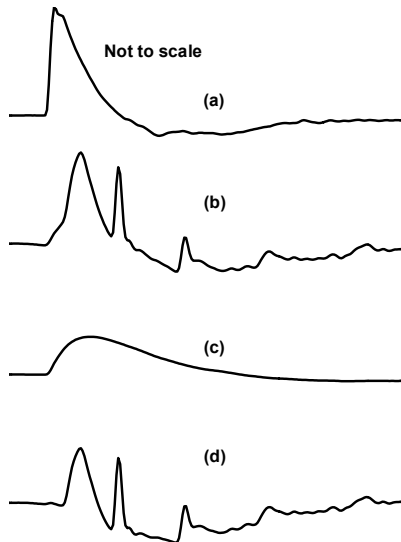


Figure 2. Shape of (a) direct, (b) total diffracted pulse sequence for 60mm gap, (c) bare and (d) total – bare. These are pressure (strictly excess pressure) time graphs.

A further problem arises for a parallel gap width of 210mm, where the result at the receiver was essentially a single very large peak sitting on the bare background. With this large gap width, a ray can be drawn from the source to the mid-point of the top surface of the gap, then reflected down at the same angle to a receiver at $\theta = 60^\circ$. Assuming the inner surfaces of the gap were perfectly hard reflectors, as the received pulse was never diffracted it should just be a copy of the incident pulse. However, it was significantly narrower. A further observation was that the bare pulse also narrowed if the receiver angle was increased beyond 90° , when the receiver was no longer in the shadow of the barrier.

Diffraction model

We have chosen to adapt the theoretical diffraction model of Medwin (Medwin, Childs and Jepsen 1982). Initially consider the situation where the ray incident at an angle ϕ onto a corner wedge of angle ψ propagates away at an angle θ to the second surface of the wedge, as occurs at the first wedge of Figure 3. In our case, ψ is always 90° .

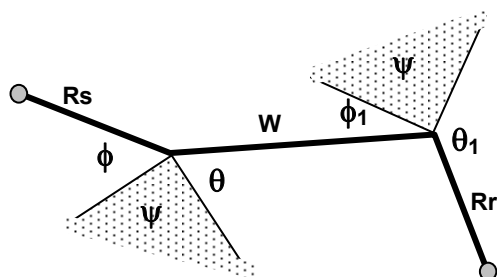


Figure 3. Geometry for serial diffraction from two wedges separated by a distance W.

The calculated polar pattern at two frequencies resulting from applying Medwin’s diffraction theory to a right-angle corner and an incident angle of 60° is shown in Figure 4. It is noticeable that as well as a broad minimum around 75° , there are two very sharp discontinuities present, in this case near 30° and 150° . In general, for an incident angle ϕ less than 90° , the discontinuities occur at $(90^\circ \pm \phi)$. Calculations involving such angles will be referred to as the “critical angle” condition.

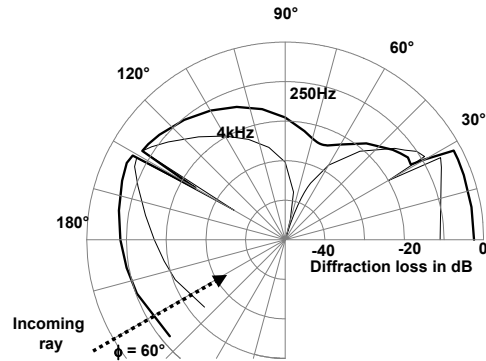


Figure 4. Polar pattern showing loss in dB as function of diffracting angle for a 90° wedge and 60° incident angle.

The discontinuities represent regions where the Medwin theory yields questionable results, making calculations unreliable in a narrow band of angles around the discontinuities. Further, there is a phase change across the discontinuity, a result not noted explicitly by Medwin. This implies that a pulse diffracted at an angle beyond the discontinuity will be inverted compared to one before the discontinuity.

For purposes of this investigation, it was also necessary to modify the Medwin theory to permit the two diffraction edges to be on different bodies separated by a distance W, as

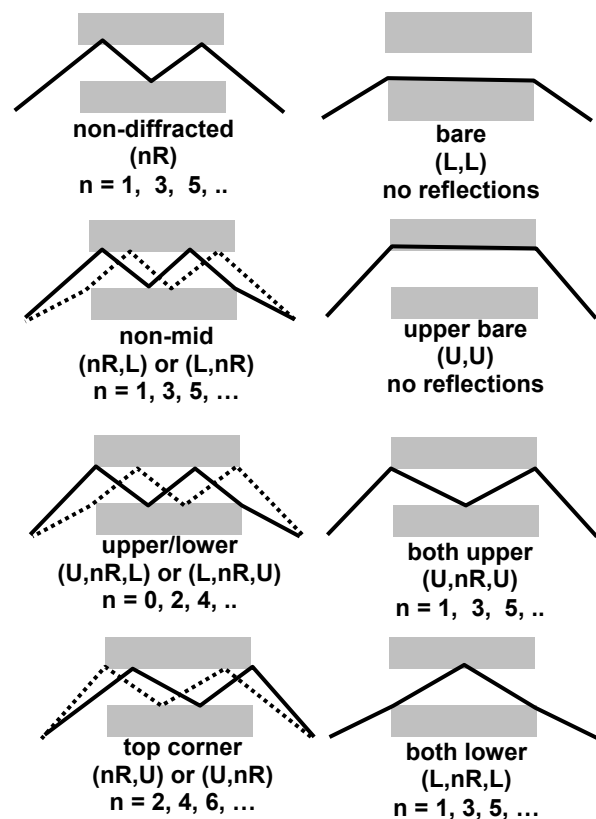


Figure 5. All possible ray paths obeying diffraction and Snellian reflection in a rectangular gap.

shown in the Figure 3. The frequency components contained in our direct pulse were multiplied by the real and imaginary coefficients from the Medwin model and an inverse FFT performed to produce the diffracted pulse.

When applying the theory to gaps, it is often convenient to refer to “ray paths” and to assume that all reflections obey Snell’s law from a perfect reflector. All the possible types of ray paths for a parallel sided gap are shown in Figure 5, together with a descriptive name for the path and a notation which indicates if the diffraction is at a lower edge (L) or an upper one (U). We assume the upper surface of the gap is that furthest from the source. Further, (nR) indicates the number of reflections occurring during passage through the gap.

RESULTS

Fixed barrier results

Consider the diffraction of a pulse over just the single wide barrier, as the receiver moves from below to above the level of the barrier top. In the shadow of the barrier, only the bare component was present and this was calculated reasonably accurately (for example Figure 6(a)) using the Medwin theory at receiver angles varying from 30° to 80°.

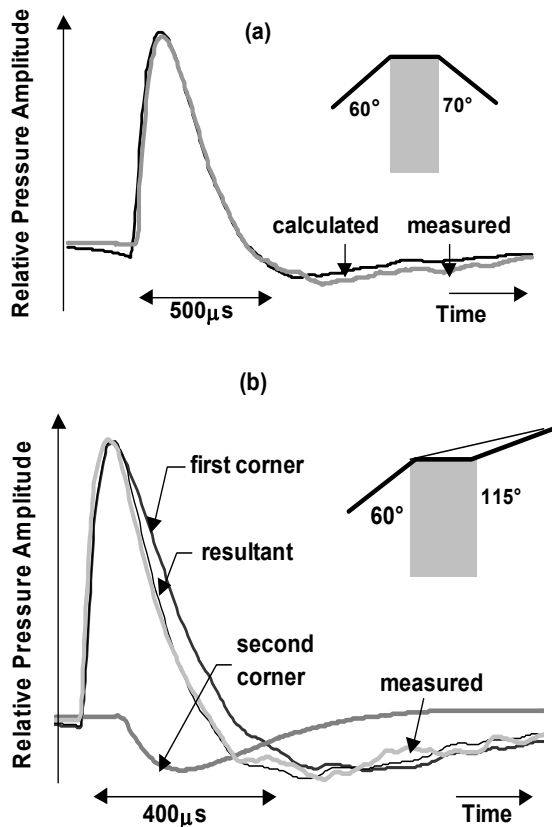


Figure 6. Comparison of a measured and calculated bare over a fixed barrier at a receiver angle of (a) 70° and (b) 115°.

Once the receiver angle increases beyond 90° the most direct path involves only diffraction at the first edge. The measured peak shape was significantly narrower than that predicted for this single diffraction, as shown in Figure 6(b). However, in this geometry there is the possibility of additional energy travelling along the barrier surface from the first edge then being diffracted upwards to the receiver from the second edge. When this component was calculated it was found to be inverted relative to the first edge component, and when appropriately delayed due to the increased path length and the

two components added, the result was in excellent agreement with the measured shape. Similar calculations performed at other receiver angles confirmed the need for inverted components to give the measured result. The overall agreement between calculation and theory in these fixed barrier cases indicated that our modifications to the Medwin approach should produce reasonable diffraction results when applied to gap geometries.

The 210mm gap results

Returning to the 210mm gap result, it is now apparent that there will be diffraction effects from each of the four edges forming the gap. Indeed, there are five main components making up the observed pulse. As well as the non-diffracted pulse reflected at the mid point of the barrier there are two “non-mid” components which reflect from points other than the middle, one diffracting at the entry edge and the other at the exit edge. Because of symmetry, each component produces the same result at the receiver and both occur 2.6µs after the non-diffracted component. Also there are two “upper/lower” components that are diffracted either at the lower then upper edge or vice-versa, again making identical contributions, delayed by 4.9µs, at the receiver. These four components are all inverted compared to the non-diffracted component. When they are all added, allowing for the different delays, the result shows a significant narrowing and agrees reasonably well with the measured pulse (Figure 7), although it has a smaller base width than the measured result.

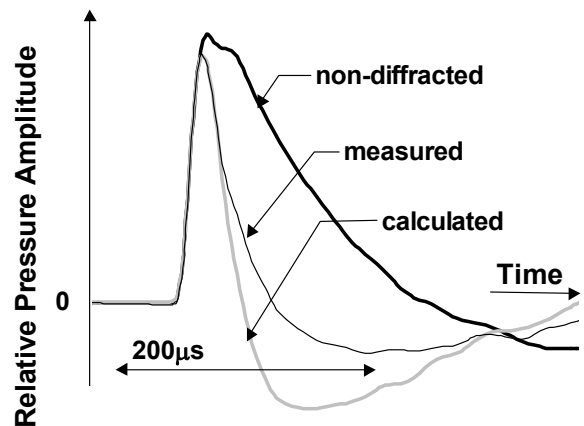


Figure 7. Diffracted pulse shapes for a gap of 210mm.

It is tempting to postulate that additional components are required to broaden the base and indeed the next two components are both upright. The (L, R, L) ray (that diffracted from the lower entry corner, then reflected from the top surface before being diffracted at the lower exit corner), reaches the receiver with a delay of 14.4µs but has an amplitude less than 1% of the non-diffracted ray. The next component to arrive, delayed by 42µs, is an “upper bare” and with an amplitude of about 2.5% of the non-diffracted component, also has only a marginal effect on the result. Other components are delayed even further and generate a small peak that cannot be distinguished in the background noise.

The “upper bare” components

The “upper bare” component occurs when sound from the source diffracts from the upper entry edge along the top inside surface to the exit edge, whence it diffracts down to the receiver. Unlike the “bare”, which is the same for any given width right-angle barrier with hard surfaces, the upper bare depends on the gap width. Figure 8 compares the bare with upper bares for various gap widths. It is apparent that as the gap width decreases, more sound energy is following this

path and this component is significantly larger than the bare itself. In the figure, all components have been aligned, however in practice the upper bares all have different path lengths and hence delays compared to the bare. Because the bare is the first component to reach a receiver behind a barrier, delayed components will be superimposed on top of it but the initial part will be clearly identifiable, as can be seen in Figure 2(b). However, the upper bare component is delayed and, although more intense, difficult to isolate in the noise of the other components.

One of the limitations of generating pulse shapes from estimated diffraction coefficients is that small distortions can arise at the start of the peak. This is apparent in the calculated curves in Figure 8, which do not instantly rise from zero.

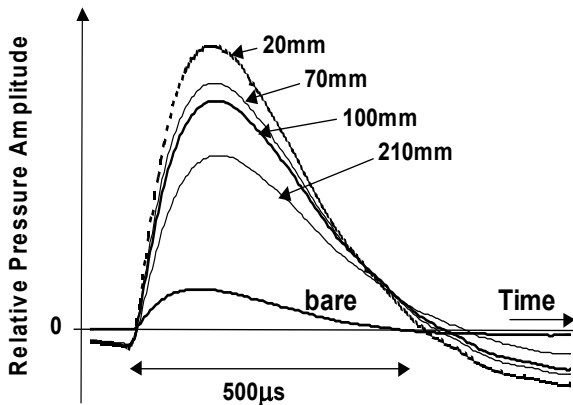


Figure 8. Comparison of the calculated bare diffraction pulse with the upper-bare results for various gap widths.

60mm gap results

As an example of calculating a sequence of pulses, consider the result for a 60mm wide parallel sided gap. After removing the bare component, measurements indicate there is a broad first peak and a very narrow second peak, then a clearly distinguished but small third peak followed by a succession of broader local maxima in the background (Figure 2(d)). One challenge is to explain the different width peaks.

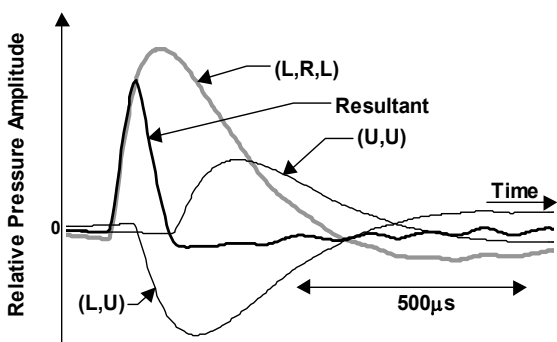


Figure 9. The three types of components of the first peak of the 60mm gap sequence and their resultant.

Calculations indicate that the first peak is formed from three different types of components, as shown in Figure 9, although the “upper/lower”, (L,U), must be doubled before adding to the others since there is another equivalent component, (U,L). The first to arrive is the “both lower” component, (L,R,L), followed 50µs later by the two (L,U) type components which have the opposite sign and so effectively curtails the first component. The upper bare component, (U,U), which arrives 77.5µs later has only a marginal effect. The

calculated resultant shape for the first peak is in quite good agreement with measurement.

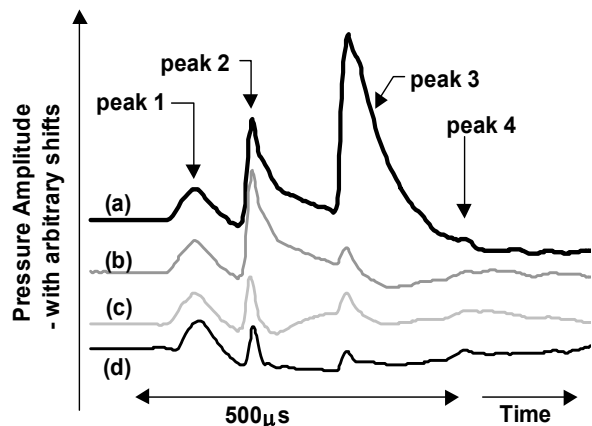


Figure 10. Calculated pulse sequences for 60mm gap (a) with no adjustments, (b) after adjusting (U,3R,U) components, (c) also adjusting (3R,L) and (L,3R) components and (d) the measured sequence.

When the first 14 components to arrive are added with appropriate delays, the result is that shown in Figure 10(a), which is dominated by the large third peak. This is caused by an intense “both upper”, (U,3R,U) component, which had to be calculated using an incident angle of 122.9° and diffraction angle of 33.5° at the entry edge and a similar combination at the exit edge. These angles are within 0.6° of the “critical angle” condition, where the Medwin theory used for calculating the component properties breaks down. Plotting a graph of the peak amplitude for (U,nR,U) components with n = 1, 5, and 7 gave rise to a smooth curve, however, the calculated value of the n = 3 peak was well away from the curve. So the probable peak value for the n = 3 case was estimated from the curve and used to adjust the (U,3R,U) amplitude. The new resultant sum is shown in Figure 10(b), which is much more realistic.

Now consider the formation of the much narrower second peak which is the result of the seven components listed in Table 1 and plotted in Figure 11. The dominant non-diffracted component is almost cancelled by two simultaneously arriving non-mid components while the slightly delayed (L,3R,L) marginally increases the result. However, it is the two upper/lower components which sharpen the resultant pulse, as shown in Figure 11, with a broadening of the base caused by the delayed and slowly rising (U,R,U) component. This calculated second peak is appropriately narrower but has a significantly greater amplitude and broader base (Figure 10(b)), than the measured result (Figure 10(d)).

Inspection of the geometry involved with the non-mid components reveals that the diffraction involves the angles of 60.0° and 31.1°, which is close to the critical angle condition where Medwin may not give correct results. Calculations were performed at a series of angles leading up to 31° and the peak value trend line suggested that the 31° non-mid peak may have been under-estimated and that a more appropriate value would be -68000 units on an arbitrary excess pressure scale. When this value was used, the resultant sum is that shown in Figure 10(c), which is a reasonable estimate of the measured signal shown as Figure 10(d).

Table 1. Properties of components forming the second peak in the 60mm gap series.

Type of component	Delay* (μs)	Peak value ¹	Rise time [#] (μs)
non-diffracted (3R)	0.0	156800	25
non-mid (3R,L) & (L,3R)	0.0	- 56200	25
both lower (L, 3R, L)	2.0	9200	35
upper/lower (U,2R,L) & (L,2R,U)	5.5	- 18100	
both upper (U, R, U)	30.5	8300	100

* delay after arrival of non-diffracted component

¹ arbitrary excess pressure units

[#] time from onset to maximum value of component

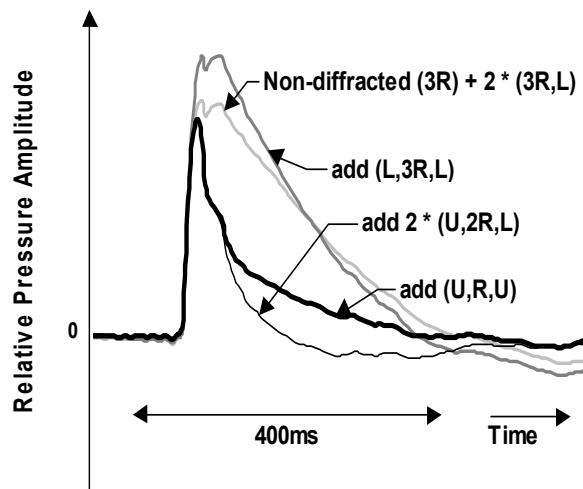


Figure 11. Formation of the second peak in the 60mm gap series without adjustment to the non-mid (3R,L) and (L,3R) components. The resultant is that shown in the top two traces of Figure 10.

The small fourth peak is formed from four much later arrivals. Initially, the “both upper”, (U,5R,U), produces a pulse in the same sense as the non-diffracted component, however, about 37μs later the two “upper/lower” components of opposite phase rapidly narrow it. A further 46μs later and the small but longer duration “both lower” pulse, which has the same sense as the “both upper”, adds to the tail.

If we let x represent the number of reflections experienced by one of the later “both upper” rays then there is a sequence of an (U,xR,U), sharpened by the two (U,{x+1}R,L) and followed by a smaller (L,{x+2}R,L) which together form a peak. This behaviour continues indefinitely, forming a sequence of progressively smaller peaks and applies to all gap widths. In practice, in generating the pulse sequence only the first one or two of these peaks would be significant.

CONCLUSION

This work has shown that a simple model involving multiple diffraction and Snellian reflection is capable of explaining the

gross quantitative behaviour of the passage of pulse sound through a simple parallel gap. What appeared initially to be single peaks have now been shown to consist of multiple components, with the phase and timing of these components being critical in determining the resultant pulse shape. Unfortunately the application of Medwin’s theory is limited at certain critical angles and interpolation techniques were required to obtain better estimates. A major assumption of this work has been lossless reflection. Allowing for this limitation could significantly improve agreement between calculation and experiment, especially as delayed components in narrow gaps experience many reflections. Now that this simple model has been used to explain parallel gap properties, it opens the possibility of extending its use to more complex geometries such as multiple slits and tapered gaps.

This paper has concentrated on predicting the time domain behaviour of the transmitted pulse. For practical purposes it will be necessary to compare our model predictions with insertion loss calculations derived from experimental results at different gap widths. Providing the agreement is reasonable, generating an appropriate pulse chain using the model considered here could provide a useful method of determining the insertion loss properties of quite complex systems that could not otherwise be calculated theoretically.

The results show that the transmitted sound is very dependent on the behaviour at the four diffracting edges. An intriguing possibility is that the sound pattern could be markedly changed if the entry and exit surfaces were contoured.

ACKNOWLEDGEMENTS

The authors would like to thank Mr. M. Butyn for his assistance with the original measurements.

REFERENCES

Don C.G., Swenson G.G. and Butyn M. (1995) *Acoustic Propagation over Barriers with Caps and Apertures.*, Conference Proceedings of the Australian Acoustics Society, Perth, WA. 15 – 17 November, pp 153-157.

Gomperts M.C. and Kihlman T. (1967) The Sound Transmission Loss of Circular and Slit-shaped Apertures in Walls, *Acoustica* 18 pp 144-150.

Horner J.L. and Peat K.S. (2006) Approximations for the Scattered Field Potential from Higher Mode Transmission in Rectangular Apertures, *Journal of Acoustical Society of America* 119(6) pp3568-3576.

Medwin H. (1981) *Shadowing by Finite Noise Barriers*, *Journal of Acoustical Society of America* 69(4) pp 1060-1064.

Medwin H., Childs E. and Jepsen G. (1982) *Impulse Studies of Double Diffraction: A Discrete Huygens Interpretation.*, *Journal of Acoustical Society of America* 72(3) pp 1005-1013.

Papadopoulos A.I. and Don C.G. (1991) *A Study of Barrier Attenuation by Using Acoustic Impulses*, *Journal of Acoustical Society of America* 90(2) pp 1011-1018.

Sauter A. and Soroka W.W. (1970) *Sound Transmission through Rectangular Slots of Finite Depth between Reverberant Rooms*, *Journal of Acoustical Society of America* 47(1A) pp5-11.